

PHYSICAL REVIEW A

ATOMIC, MOLECULAR, AND OPTICAL PHYSICS

THIRD SERIES, VOLUME 41, NUMBER 1

1 JANUARY 1990

Pion transfer from hydrogen to deuterium in $H_2 + D_2$ gas mixtures

P. Weber, D. S. Armstrong,* D. F. Measday, A. J. Noble, and S. Stanislaus†
University of British Columbia, Vancouver, British Columbia, Canada V6T 2A6

M. R. Harston
University of Surrey, Guildford, Surrey GU2 5XH, United Kingdom

K. A. Aniol
California State University, Los Angeles, California 90032

D. Horváth
*Central Research Institute for Physics, H-1525 Budapest, Hungary
and TRIUMF, Vancouver, British Columbia, Canada V6T 2A3*
(Received 5 June 1989)

The transfer of negative pions from pionic hydrogen to deuterium has been investigated in gas mixtures of H_2 and D_2 as a function of the D_2 concentration (C). The concentration dependence of the transfer rate was fitted using a phenomenological model with two parameters. For $C \rightarrow \infty$ (32 ± 3)% of the pions undergo transfer. The fitted parameters reflect the ratio of pion capture to pion transfer in collisions of pionic hydrogen with protons or deuterons. No pressure dependence for pion transfer was found.

I. INTRODUCTION

The stopping of negative charged particles such as pions and muons has been widely investigated during the past 30 years. The interplay between molecular, atomic, and nuclear interactions as well as the main features have been reviewed by Ponomarev¹ and Horváth.² Although a large amount of data has been collected, the understanding is still on a phenomenological level. Several models have been formulated for different materials with varying success.³⁻⁵ For binary compounds such as $Z_m H_n$, where H denotes hydrogen, Z the heavier element with nuclear charge Z , and m and n the stoichiometric numbers in the molecule, Ponomarev invented the model of large mesic molecules⁶ (LMM), which reproduces the observed sharp Z^{-3} dependence for the capture probability W_H of stopped π^- mesons in hydrogen. The Z^{-3} dependence was originally attributed to pion transfer, i.e., the collisionally induced exchange of the pion from one atomic constituent to another. The LMM model also includes molecular effects, which became evident in the experimental ratio of pion charge exchange probabilities in hydrogen for $H_2 + N_2$ and for hydrazine, $W(2H_2 + N_2)/W(N_2H_4) \sim 30$.⁷ In a less dramatic way the molecular effect was also found by Aniol *et al.*⁸ for $H_2 + D_2$ and

HD , where $W(H_2 + D_2)/W(HD) = 1.23 \pm 0.03$ was measured.

The pion transfer reaction $\pi^- p + Z \rightarrow \pi^- Z + p$ has been systematically studied in gas mixtures of $H_2 + Z$ by measuring the concentration dependence of pion charge exchange probabilities in hydrogen. Monatomic noble gases like He, Ne, Ar, Kr, and Xe (Refs. 9 and 10) (where there are no chemical bond effects) were added to hydrogen, as well as simple molecules such as D_2 ,¹¹ N_2 , CO , and CO_2 ,^{10,12} and also polyatomic molecules.¹³ For all Z , the pion transfer probability exceeded 90% for impurity concentrations $C > 1$. This is still considerably less than for muons,¹ but nevertheless quite significant remembering that the lifetime of the πp atom is relatively short, $\sim 2 \times 10^{-12}$ s,¹⁴ in comparison to the μp atom, $\sim 2 \times 10^{-6}$ s, which thus allows far more time for transfer. For polyatomic gases a maximum showed up for the pion charge exchange probability in hydrogen at small concentrations $C \sim 0.1$.¹⁵ This was in line with the earlier observation that pion capture is not proportional to the partial stopping powers of a mixture.¹⁵

Among all the investigated $H_2 + Z$ gas mixtures, the $H_2 + D_2$ system is a special case, as $Z = 1$ for both hydrogen and deuterium. Both pionic hydrogen $\pi^- p$ and pionic deuterium $\pi^- d$ are neutral, which facilitates free

movement through other atoms and molecules. In a $H_2 + D_2$ mixture the transfer reaction is



Because Z is the same for both hydrogen and deuterium, pion transfer was expected to be much smaller than for the impurities with higher Z , and the inverse transfer reaction



was also considered to take place. Experimentally, pion transfer in $H_2 + D_2$ gas mixtures was first measured by Petrukhin and Prokoshkin.¹¹ At large D_2 concentrations pion transfer was observed to be $(23 \pm 4)\%$, significantly smaller than in mixtures with heavier impurities Z . From the observed concentration dependence the inverse transfer reaction was concluded to be of comparable importance to (1). However, the quality of the data was worse than those of the noble gases, as small differences had to be measured due to the smaller transfer probability.

Substantial interest in pion transfer in mixtures of hydrogen isotopes arises from muon-catalyzed fusion.¹⁶ Good experimental data¹⁷ and theoretical calculations¹⁶ exist on muon transfer from the ground state ($1s$), as measured in low-pressure gas targets. At conditions with increased pressure muon transfer reactions from excited states nS such as $(\mu^- d)_n + t \rightarrow (\mu^- t)_n + d$ become important. As it turns out, the study of muon transfer from excited states is not trivial, because the muonic hydrogen can deexcite to the ground state or any excited level and competitive processes such as thermalization and acceleration in collisions take place.¹⁸ Therefore, pion transfer in gaseous mixtures of hydrogen isotopes becomes interesting for application to muon-catalyzed fusion, as here it is known that the transfer has to occur at excited states with $n=4$ or 5 . This constraint is known both from cascade calculations and the nuclear capture rate in hydrogen. External Auger deexcitation dominates the energy loss for highly excited pionic hydrogen ($n > 5$) and nuclear capture prevails for $n \leq 3$ ($\Gamma_{ns} \sim 1.5 \times 10^{15}/n^5 \text{ s}^{-1}$). Therefore, the two processes limit the transfer reactions to $n=4,5$.

Pion capture is commonly studied by means of pionic x rays. The detection of x rays from pionic hydrogen or pionic deuterium in the energy region of a few keV is very difficult, especially in a high-pressure gas target. In hydrogen, the branching ratio for the nuclear capture reactions is well known,¹⁹

$$\pi^- p \rightarrow \pi^0 n, \quad \pi^0 \rightarrow 2\gamma \quad (\sim 60\%), \quad (3)$$

$$\pi^- p \rightarrow \gamma n \quad (\sim 40\%). \quad (4)$$

Detection of the π^0 from the charge exchange reaction (3) offers an alternative technique which works out very well, because the observation of a π^0 following pion capture is a very clean signature that the pion was captured by hydrogen. Except for ${}^3\text{He}$, with a branching ratio of $\sim 13\%$ for $\pi^- {}^3\text{He} \rightarrow \pi^0 t$ at rest,^{15,20} π^0 production in any other nucleus ($A > 3$) is strongly suppressed ($< 10^{-5}$),²¹

mainly by energy conservation. This fact is very important because the measurement of π^0 's is practically free of any background stemming from stopping π^- captured in atoms other than hydrogen. The suppression of charge exchange for stopped pions in deuterium,²² $\sim (1.45 \pm 0.19) \times 10^{-4}$, is crucial for the technique in this experiment. It is not forbidden by energy conservation, but by the Pauli principle which excludes the $\pi^0 nn$ final state with $L_{nn} = 0$.

Pion transfer from hydrogen to higher- Z nuclei can be examined by the reduction in π^0 yield compared to the pure hydrogen target as the concentration of Z is increased.

II. PHENOMENOLOGICAL MODEL

The phenomenological model of large mesic molecules by Ponomarev⁶ comprises three probabilities for the charge exchange reaction $\pi^- p \rightarrow \pi^0 n$ in binary compounds of $Z_m H_n$, given by

$$W_H = W_1 W_2 W_3, \quad (5)$$

where W_1 is the probability of pion capture in a mesomolecular orbit, W_2 is the probability of a transition to an atomic orbit, and W_3 is the probability that the pion will be captured by a proton and not transferred to Z . The model assumes that pions first undergo Coulomb capture in a mesomolecular state $HZ\pi^-$. Isolated pionic atoms such as $\pi^- p$ or $\pi^- Z$ are the consequence of deexcitation, mainly by emission of Auger electrons. At this stage pion transfer can occur in collisions $\pi^- p + Z \rightarrow \pi^- Z + p$, competing with nuclear capture. It is quite obvious that the pion transfer reaction in compounds of $Z_m H_n$ is different from that in gas mixtures of $H_2 + Z$. Internal transfer can be responsible for pion transfer in $Z_m H_n$ compounds, whereas only external transfer can occur in $H_2 + Z$ mixtures, when a π^- is transferred from p to Z .

In Fig. 1, a schematic rate diagram exhibits the fate of

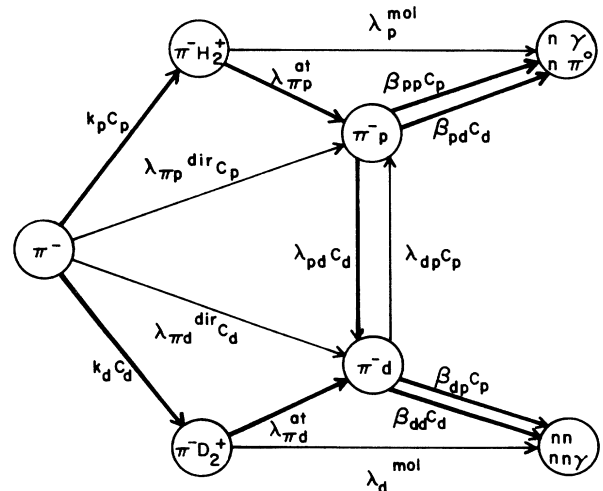


FIG. 1. Schematic rate diagram of stopping π^- in H_2 and D_2 . All symbols associated with the arrows are explained in the text.

stopping pions in $H_2 + D_2$ mixtures. The symbols used in Fig. 1 for the rates λ , β , and k have the following meaning: $\lambda_p^{\text{mol}}(\lambda_d^{\text{mol}})$, direct nuclear capture from mesomolecular states of hydrogen (deuterium); $\lambda_{\pi p}^{\text{dir}}(\lambda_{\pi d}^{\text{dir}})$, direct atomic capture of pion on hydrogen (deuterium) atom; $\lambda_{\pi p}^{\text{at}}, \lambda_{\pi d}^{\text{at}}$, transition from mesomolecular state to atomic orbital; λ_{pd} , pion transfer from p to d in collision with d ; λ_{dp} , pion transfer from d to p in collision with p ; $\beta_{pp}C_p$, nuclear capture rate $\pi^-p \rightarrow \pi^0n$ or γn in $\pi^-p + p$ collision; $\beta_{pd}C_d$, nuclear capture rate $\pi^-p \rightarrow \pi^0n$ or γn in $\pi^-p + d$ collision; $\beta_{dp}C_p$, nuclear capture rate $\pi^-d \rightarrow nn$ or γnn in $\pi^-d + p$ collision; $\beta_{dd}C_d$, nuclear capture rate $\pi^-d \rightarrow nn$ or γnn in $\pi^-d + d$ collision; k_pC_p , initial molecular capture rate on H_2 ; k_dC_d , initial molecular capture rate on D_2 ; where C_p and C_d are the relative hydrogen and deuterium concentration, respectively.

The rate diagram of Fig. 1 can be used to formulate relations for the nuclear capture probability in hydrogen, $W_{H_2D_2}$, and the transfer Q in a phenomenological manner. Only two parameters κ and Λ are introduced to describe the concentration dependence of $W_{H_2D_2}$ and Q . In order to simplify the expression (6), we assume that the direct nuclear capture rate from mesomolecular states is small, i.e., $\lambda_p^{\text{mol}} \ll \lambda_{\pi p}^{\text{at}}$ and $\lambda_d^{\text{mol}} \ll \lambda_{\pi d}^{\text{at}}$. We also ignore direct atomic capture. The nuclear capture probability in hydrogen can then be written for a mixture of hydrogen and deuterium as^{10,11}

$$W_{H_2D_2} = \frac{k_p C_p}{T} \frac{\beta_{pp} C_p + \beta_{pd} C_d}{\beta_{pp} C_p + \beta_{pd} C_d + \lambda_{pd} C_d} + \frac{k_d C_d}{T} \frac{\lambda_{dp} C_p}{\beta_{dp} C_p + \beta_{dd} C_d + \lambda_{dp} C_p}, \quad (6)$$

where T stands for $k_p C_p + k_d C_d$. Assuming $k_d/k_p \sim 1$ it follows that

$$W_{H_2D_2} = \frac{(1 + \kappa C)}{(1 + C)(1 + \kappa C + \Lambda C)} \quad (7)$$

if the inverse transfer rate λ_{dp} is small. Justification for this assumption can be found in Ref. 23, where the pion transfer reaction $(\pi^-p)_n + d \rightarrow (\pi^-d)_n + p$ is treated as a quaresonance one with a resonance defect $\Delta u \sim 235$ eV/ n^2 . Consequently, for the inverse pion transfer from pionic deuterium to the proton, a kinetic energy of ~ 10 eV ($n=4,5$) is needed to surpass the resonance defect.

In expression (7) $C = C_d/C_p$ is the concentration ratio, $\kappa = \beta_{pd}/\beta_{pp}$ is the ratio of nuclear capture in $\pi^-p + d$ to $\pi^-p + p$ collisions, and $\Lambda = \lambda_{pd}/\beta_{pp}$ is the ratio of transfer probability in the $\pi^-p + d$ collision to the nuclear capture probability in the $\pi^-p + p$ collision. The ratio $\kappa/\Lambda = \beta_{pd}/\lambda_{pd}$ is the ratio of nuclear capture probability to transfer probability in $\pi^-p + d$ collisions.

Similarly the transfer Q , describing the transfer of π^- from hydrogen to deuterium in $\pi^-p + d$ collisions, can be written as

$$Q = \frac{\lambda_{pd} C_d}{\lambda_{pd} C_d + \beta_{pp} C_p + \beta_{pd} C_d} = \frac{\Lambda C}{1 + \kappa C + \Lambda C}, \quad (8)$$

again neglecting the inverse transfer rate λ_{dp} .

$W_{H_2D_2}$ and Q are simply related by the expression

$$W_{H_2D_2} = \frac{1 - Q(C)}{(1 + C)}. \quad (9)$$

The measurement of the π^0 yield for various concentrations of H_2 and D_2 allows the determination of $W_{H_2D_2}$ and Q . From both observables the concentration dependence yields the parameters κ and Λ by fitting function (7) to the measurements.

III. EXPERIMENT

The experiment was performed at TRIUMF using the M9 stopped π/μ channel for one set of data and the M13 low-energy pion channel for another data set. The experimental setup is depicted in Fig. 2. A high-pressure gas target [Fig. 3(a)], operating at 100 atm, was employed to stop the pions in the mixture of hydrogen and deuterium. Its design and characteristics are a compromise of target-gas pressure and target-wall thickness in order to stop as many pions as possible in the gas, yet to minimize the amount of material for the γ rays from the π^0 decay to traverse. The target vessel itself was turned from an aluminum alloy with excellent strength-to-weight ratio. The thickness of the aluminum walls was 0.8 cm. The brass flanges formed a seal against the vessel and the light guides. External clamps were fastened to the light guides to prevent inward movement when the target was under vacuum. The scintillation counters S_3 and S_4 were placed inside the aluminum target vessel [see Fig. 3(a)] to obtain a meaningful stop definition for the pions. S_3 was made of a very thin (0.5 mm) deuterated plastic $(CD)_n$ to reduce the hydrogenous background and to minimize the number of stops in the scintillator itself. S_4 was a 0.32-cm-thick ordinary plastic scintillator of closed cylinder shape with one face open. The geometry of S_3 and S_4 [Fig. 3(b)] constrained the pions to stop in the enclosed gas volume if the stop definition was fulfilled. Both S_3 and S_4 were covered with aluminum foil to avoid light transfer between the two counters.

99.999% pure H_2 , 99.6% enriched D_2 , and mixtures of $H_2 + D_2$ at various concentrations served as targets. Be-

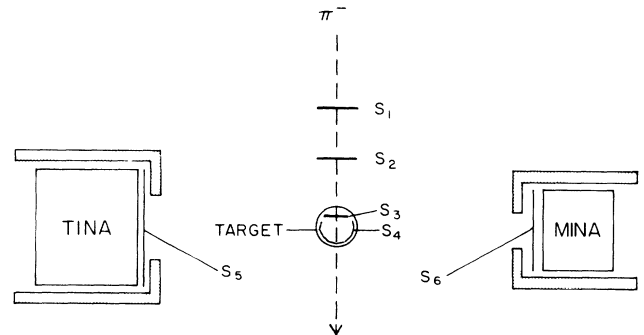


FIG. 2. Experimental setup. S_1 – S_6 are plastic scintillation counters. TINA and MINA are the NaI crystals detecting the γ rays from the π^0 decay. The boxes around TINA and MINA shield from background and define the aperture.

cause of the high stability requirement of the measurement, cycles of two different $H_2 + D_2$ concentrations were measured, followed by a pure H_2 run. The π^0 background was studied with D_2 and N_2 serving as the target gas. Data were also taken with an evacuated target several times to determine and monitor the fraction of pions stopping in the scintillator S_3 . The gas mixture of a given concentration C was prepared in a mixing vessel, using a Varian strain gauge transducer to measure the gas pressure, accurate to better than 0.05%. Sufficient time had to be allowed as the gas cooled down after filling, and consequently led to a drop in the pressure. We also found that the gases did not mix quickly so the mixture was pumped in and out of the target to ensure a uniform mixing. The target was filled to 100 atm for all mixtures by means of a compressor. After each measurement the target was evacuated, the gas in the mixing vessel further diluted with H_2 to another concentration, or the target was filled with pure H_2 .

The concentration of the gas mixture is given by the partial pressure of H_2 and D_2 , i.e.,

$$C = \frac{n_d}{n_p} = \frac{P_{D_2}}{P_{H_2}}. \quad (10)$$

Expression (10) holds only for ideal gases and hence the virial corrections have been included to account for the

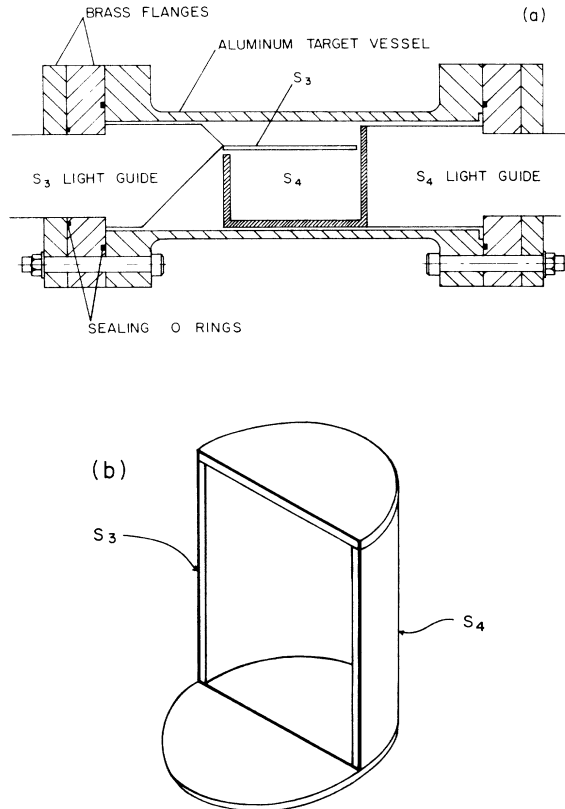


FIG. 3. (a) Detailed view of the high-pressure gas target. (b) Detailed sketch of scintillators S_3 and S_4 .

nonideal behavior of the gas at high pressure. The second virial coefficient was calculated, neglecting higher-order coefficients. A more detailed description can be found in Ref. 8 and references therein.

The precision in the gas mixture was a crucial point for the analysis of the data. In some cases samples of measured $H_2 + D_2$ mixtures were taken and analyzed with a quadrupole mass analyzer. The analysis of the concentration C was found to be in agreement with the direct determination using the Varian strain gauge transducer. Hence we assume the concentration to be known to be better than 1%.

The π^- beam with an incident momentum of 78 MeV/c passed through the beam counters S_1 , S_2 , and S_3 (see Fig. 2) and stopped in the target. The electrons and muons in the beam passed through the target without stopping. A coincidence of S_1 , S_2 , and S_3 signaled the arrival of a particle and the veto counter S_4 was used to check the stopping of the particles in the target. The π^0 detection technique was very similar to the one described in detail by us earlier.²⁴ Two large NaI detectors TINA (ϕ 46 cm \times 51 cm) and MINA (ϕ 36 cm \times 36 cm) were used in coincidence to detect the two γ rays from the decay of the π^0 . The π^0 detection system had an efficiency of $\sim 10^{-3}$. A π^0 -related event was triggered by a coincidence of S_1 , S_2 , S_3 , TINA, and MINA. A signal in the plastic scintillators S_5 or S_6 (Fig. 2) identified a charged particle incident on TINA or MINA, in which case the event was rejected. The time of flight of the particles incident on TINA and MINA was recorded in order to distinguish γ rays from neutrons. The rejection of both charged particles and neutrons was done in the software during the off-line analysis.

The beam composition of pions, muons, and electrons was monitored by measuring the time of flight of the beam particles with respect to the rf signal of the cyclotron, by triggering events with random coincidences of S_1 , S_2 , and S_3 with a pulse generator. The composition of the particles stopping in the target was deduced from the same random events by using the additional information from the S_4 veto counter. 30% of the pions were stopped in the target gas, which corresponds to $\sim 3\%$ of the beam particles. The data acquisition was performed using a PDP-11/34 computer with the MULTI²⁵ program package.

IV. DATA ANALYSIS

The π^0 -related events were selected by using techniques described and illustrated in detail in Ref. 24. A histogram of $E_T E_M$, where E_T is the energy deposited in TINA and E_M is the energy deposited in MINA, was generated to determine the π^0 yield N_{π^0} . Since

$$E_T E_M = \frac{M_{\pi^0}^2}{4 \sin^2(\psi/2)}, \quad (11)$$

where M_{π^0} is the mass of the π^0 and ψ is the angle between the two γ rays detected in TINA and MINA, the π^0 events show up as a peak in this histogram. A typical $E_T E_M$ histogram is illustrated in Fig. 4. The width of the

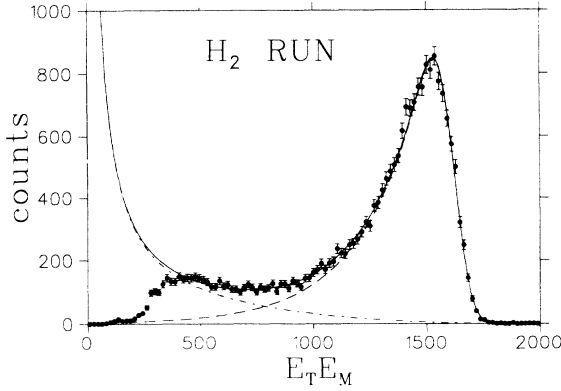


FIG. 4. π^0 energy spectrum for a pure H_2 run as measured in TINA and MINA. The dashed curve is the fitted π^0 spectrum, the dashed-dotted line is the background term, and the solid line is the sum of the π^0 spectrum and the background term as described in the text.

peak is mainly caused by the energy resolutions of the two detectors, which were about 6–8% full width at half maximum (FWHM) at 100 MeV. The number of π^0 's for each target was determined by fitting a function

$$F(E) = A \exp \frac{(E-B)}{D} \left[1 - \operatorname{erf} \frac{(E-B)}{C} \right] + BG, \quad (12)$$

where $E = E_T E_M$ and $BG = aE + bE^2 + c/E + f$ is a background term. A (normalization), B (peak position), C (right halfwidth), and D (left halfwidth) are parameters related to the π^0 peak and a , b , c , and f are parameters related to the background. The program MINUIT²⁶ was employed for the fitting procedure. The result of the fit is drawn as a solid line in Fig. 4. Integration of the π^0 peak above the background gave N_{π^0} . For most runs with pure H_2 and $H_2 + D_2$ mixtures the number of π^0 's in the peak far exceeded 10^4 events, which is equivalent to a statistical uncertainty of $<1\%$. The analysis of the runs with the target evacuated provided an $E_T E_M$ spectrum compatible with zero π^0 's, i.e., in the region of interest there were only a few counts. However, the π^0 spectrum for the pure D_2 runs exhibited a peak which contains almost 1% of a pure H_2 run. The presence of π^0 's at this level cannot be explained from the reaction $\pi^- + d \rightarrow \pi^0 nn$, which contributes to the peak only $\sim 0.025\%$ of a pure H_2 run. However, the π^0 background can be partly attributed to the H_2 impurity in the D_2 gas (99.6%), which can account for as much as 0.4%. The remaining π^0 background of the same order of magnitude can be explained by charge exchange of stopped π^- in the surface of the scintillator S_4 (which was made out of ordinary plastic), the light output being too small and therefore not triggering the veto counter. It is interesting to note that this effect was not observed with the evacuated target. Of course it could be argued that the stopping π^- enter S_4 with a higher momentum because they would not be slowed down by the presence of target gas, and thus produce sufficient light to trigger the veto counter. The analysis of the N_2 run did not reveal

any π^0 's. Because of the higher density of N_2 compared to the hydrogen isotopes, all pions would have stopped in the N_2 gas and therefore would not have reached the veto-counter S_4 , the origin of this small π^0 background contribution. An upper limit of 7×10^{-5} (90% confidence level) can be given for the π^0 production in N_2 , which is exothermic by 3.94 MeV. Despite this slight puzzle, the π^0 background of $<1\%$ for the pure D_2 runs is not serious and was easily subtracted for each run. No further corrections have been applied to the N_{π^0} data.

In order to determine the relative charge exchange probability $W_{H_2 D_2}$ at various concentrations, the number of π^- mesons stopping in the target, N_{π^-} , is required. For each target this number was calculated from

$$N_{\pi^-} = S_{123} f_{\pi^-}, \quad (13)$$

where f_{π^-} is the fraction of pions (out of total incident particles) that stop in the target and S_{123} is the total number of particles incident on the target. S_{123} was counted and recorded during the experiment as a CAMAC scaler. The quantity f_{π^-} was found using the beam samples from the pulser strobe. In addition, N_{π^-} , the number stopping, has been corrected for the π^- fraction stopping in S_3 , as determined from the vacuum runs.

The absolute charge exchange probability in hydrogen is given by the Panofsky ratio $W_H = (0.607 \pm 0.004)$.¹⁹ Using W_H and the ratio N_{π^0}/N_{π^-} for a pure hydrogen run, the π^0 acceptance of the detector system can be calculated. However, as the π^0 acceptance was kept constant during the whole experiment the relative charge exchange probabilities $P(C) = N_{\pi^0}/N_{\pi^-}$ for any concentration C can be directly compared to the pure hydrogen runs with $P(C=0)$. $P(C=0)$ was determined as the weighted mean from all measurements with pure hydrogen.

In the present experiment the concentration dependence of the pion transfer $Q(C)$ was measured at the 100 atm pressure of the target gas. It is conceivable that Q depends also on the pressure itself. In order to pursue such an effect, the pressure of the target gas was lowered for just one concentration, $C=1.216$. Data were taken at 100, 66, and 33 atm. As the pressure was lowered N_{π^-} gradually decreased as well, i.e., the stopping fraction f_{π^-} was proportional to the pressure. The measurement and the analysis were the same as described above for the standard pressure choice of 100 atm.

In the present paper results are presented from two independent experiments, labeled I and II in the following. These two experiments were conducted at different times on two different beam lines at TRIUMF but using the same apparatus and data collection techniques. Dictated by the smallness of $Q(C)$, a high stability of the beam and small statistical and systematic uncertainties were required in order to obtain an accurate concentration dependence. The achieved statistical accuracy of better than 1% is difficult to improve and would be extremely time consuming. The π^0 background from the scintillator S_4 and the hydrogen contamination in the D_2 gas can

be determined and subtracted sufficiently well. Also it is hard to improve one's knowledge of the concentration C , as the pressure gauge calibration as well as the temperature effect during the mixing procedure introduce a systematic error.

A bigger problem was related to the stability of the beam, i.e., the knowledge of N_{π^-} . The stability can be inferred from the reproducibility of N_{π^0}/N_{π^-} for pure H_2 runs, which is $<2\%$ for data set I and $\sim 4\%$ for data set II. This fluctuation is significantly larger than the statistical uncertainty from the π^0 peak ($<1\%$) and has to be attributed to the counting of stopping π^- . The light output of the deuterated, 0.5-mm-thick scintillator S_3 was very small so that it gave small signals even for the very high voltages applied to the photomultiplier tube. Electrons produced a signal just above the hardware threshold of the discriminator. A slight change in gain of S_3 would affect the counting of electrons and consequently change the fraction of pions out of the total beam particles. A similar argument holds for S_4 . To study this effect, data were taken detecting all beam particles and also with a hardware threshold set above the electrons. The change in hardware threshold was made in the discriminator for scintillator S_2 , which was thick enough for a clean separation of electrons and pions.

We also attempted to analyze the data assuming that f_{π^-} remains constant and therefore $N_{\pi^-} = S_{123} \times \text{const.}$ The latter method can be directly compared to N_{π^-} as obtained from Eq. (13) when using the pulser events. The reproducibility of N_{π^0}/N_{π^-} was the criterion to favor one method over the other. The two best data sets are presented, I with a hardware threshold below the electrons and assuming constant f_{π^-} , and II with a hardware threshold above the electrons and f_{π^-} independently determined in each run.

V. RESULTS AND DISCUSSION

To obtain a measure of pion transfer from the proton to the deuteron, the relative charge exchange probability $W_{H_2D_2}$ can be studied as a function of the deuterium concentration $C_d = \rho_d / (\rho_d + \rho_p)$. By definition $W_{H_2D_2}(C_d=0)=1$ for pure hydrogen, and $W_{H_2D_2}(C_d=1) \sim 0$ reflects the suppression of charge exchange probability in deuterium, being $(1.45 \pm 0.19) \times 10^{-4}$.²² The results are given in Table I, listed as a function of $C = C_d / (1 - C_d)$. Figure 5 displays $W_{H_2D_2}(C_d)$. The errors given for $W_{H_2D_2}$ consist of the statistical uncertainty of N_{π^0} , the normalization error $\Delta W_{H_2D_2}(C_d=0)$ introduced by the reference target of pure H_2 , and a small error from the concentration. The dashed line in Fig. 5 connects the two extremes $W_{H_2D_2}(C_d=0)$ and $W_{H_2D_2}(C_d=1)$ and indicates the expected charge exchange probability if no transfer occurs. Obviously all data points lie below the dashed line, indicating pion transfer from π^-p to d . A quantitative analysis of the transfer parameters can be obtained by fitting the data to the phenomenological model, as derived in Eqs. (6)–(9).

TABLE I. Summary of charge exchange probabilities $W_{H_2D_2}$ and transfer Q as a function of the concentration C (the error on the concentration is less than 1%).

Concentration C	$W_{H_2D_2}$	$Q(C)$
data I		
0.0	1.000±0.018	0.000±0.020
0.209	0.760±0.014	0.081±0.017
0.413	0.598±0.017	0.155±0.026
0.528	0.534±0.010	0.184±0.015
0.623	0.502±0.013	0.186±0.022
0.828	0.431±0.010	0.213±0.020
0.832	0.444±0.011	0.187±0.021
1.216	0.357±0.008	0.209±0.018
2.237	0.223±0.005	0.277±0.020
2.573	0.194±0.004	0.307±0.021
2.733	0.201±0.005	0.248±0.022
5.295	0.138±0.003	0.129±0.062
5.384	0.116±0.003	0.262±0.031
data II		
0.094	0.857±0.045	0.062±0.049
0.301	0.663±0.040	0.137±0.053
0.315	0.684±0.029	0.101±0.039
0.421	0.637±0.034	0.095±0.048
0.525	0.552±0.033	0.158±0.050
0.830	0.453±0.025	0.171±0.046
1.039	0.416±0.013	0.151±0.027
1.219	0.376±0.020	0.166±0.045
1.592	0.300±0.018	0.222±0.047
3.075	0.188±0.013	0.234±0.053
4.064	0.134±0.008	0.321±0.041
4.188	0.142±0.008	0.263±0.042
6.322	0.097±0.007	0.290±0.051
6.388	0.096±0.006	0.291±0.045
7.766	0.086±0.005	0.246±0.044
8.513	0.078±0.005	0.258±0.048
8.722	0.076±0.005	0.261±0.049

The percentage of transfer as a function of the concentration $C = \rho_d / \rho_p$ is more obvious if $Q(C) = 1 - (1 + C)W_{H_2D_2}$ is plotted. This simple transformation of the relative charge exchange probability yields the data points in Fig. 6. Here $Q(C=0)=0$ stands for the case of pure hydrogen and $Q(C \rightarrow \infty)$ gives the asymptotic value for transfer from π^-p to d . The values for $Q(C)$ are also given in Table I. In both Figs. 5 and 6 the solid circles belong to data set I and the open circles to data set II. The size of the error bars, which is generally smaller for set I compared to set II, is governed by the accuracy of $W_{H_2D_2}(C=0)$. The value for Q at $C=5.295$ from set I is too low by a factor of 2, as can be seen from Table I. This data point has been taken next to a pure hydrogen run which was also in disagreement with the general trend. A concentration error is quite improbable because the consecutive run with diluted $H_2 + D_2$ gave a good agreement. Therefore the fluctuation has to be attributed to a beam instability and consequently the point has been discarded from the analysis and is not shown in Figs. 5

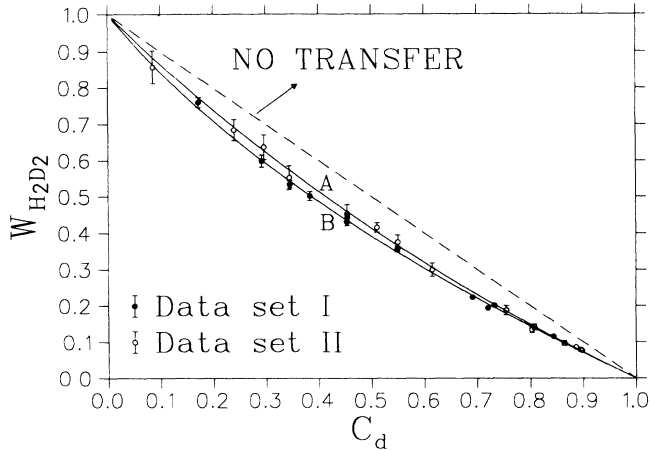


FIG. 5. Relative charge exchange probabilities $W_{H_2D_2}$ as a function of the deuterium concentration C_d . The solid circles are from data set I with fit marked A and the open circles are from data set II with fit marked B. The function $Q = (1 + \kappa C)/(1 + C)/(1 + \Lambda C + \kappa C)$ has been fitted to the data with $\Lambda = 0.71$ and $\kappa = 1.56$ for fit A, and $\Lambda = 0.40$ and $\kappa = 0.91$ for fit B.

and 6. However, the hydrogen run in question has been included to determine the error $\Delta W_{H_2D_2}$.

The remaining values were fitted to the function (7) to obtain the parameters Λ and κ using the program MINUIT.²⁶ We present the results of the fit independently for both data sets,

$$\Lambda = 0.71 \pm 0.09, \quad 0.40 \pm 0.10,$$

$$\kappa = 1.56 \pm 0.28, \quad 0.91 \pm 0.20,$$

for data sets I and II, respectively. The error bars for Λ and κ result from MINUIT too. The χ^2/df of the fits were 1.9 and 0.5 for the two fits, respectively, indicating that the error bars for data set I may have been slightly underestimated and the opposite holds for data set II. For illustration both fits are drawn in Fig. 5 as solid lines and in Fig. 6 as dashed lines. Although Λ and κ differ considerably for the two data sets, the two curves are similar, which is consistent with the good overall agreement of the two data sets. The difference of Λ and κ simply reflects the fact that the "slope parameter" Λ depends critically on the region of low concentration C , where the data points of set I are a little higher. If the ratio κ/Λ is formed then we obtain very consistent results, i.e., $\kappa/\Lambda = 2.2 \pm 0.5$ and 2.3 ± 0.8 for sets I and II, respectively. This ratio is in line with the asymptotic values $Q(C \rightarrow \infty) = \Lambda/(\Lambda + \kappa)$, which are $(31 \pm 3)\%$ and $(30 \pm 4)\%$ for the two data sets, respectively. As the errors of the parameters Λ and κ are strongly correlated and the ratio κ/Λ is quite stable, it is more realistic to determine the uncertainty $\Delta Q(C \rightarrow \infty)$ from the systematic error introduced by the normalization for pure hydrogen ($< 2\%$ and $\sim 4\%$ for data set I and II, respectively). Because the relative charge exchange probability $W_{H_2D_2}(C)$ for any concentration is given by $P(C)/P(0)$, the normalization error enters linearly and largely deter-

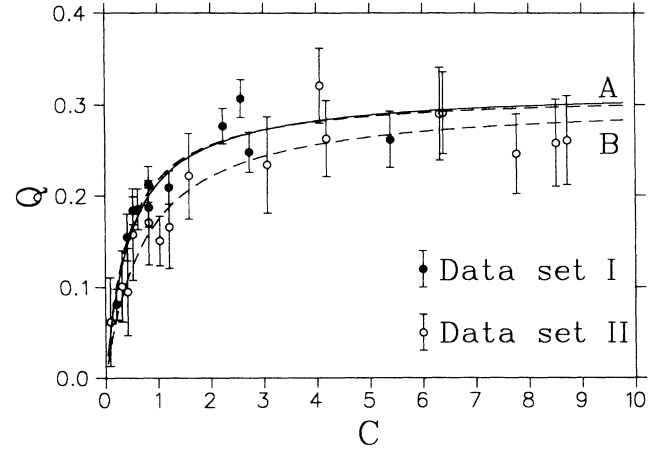


FIG. 6. Transfer probability Q as a function of C . The solid circles are from data set I and the open circles are from data set II. The solid line is the result from fit I+II, the dashed lines refer to the individual fits of data set I (curve A) and II (curve B), respectively. The function $Q = \Lambda C/(1 + \Lambda C + \kappa C)$ has been fitted to the data with $\Lambda = 0.71$ and $\kappa = 1.56$ for fit A, $\Lambda = 0.40$ and $\kappa = 0.91$ for fit B, and $\Lambda = 0.65$ and $\kappa = 1.40$ for fit I+II.

mines the error bars of the present data points and consequently also $\Delta Q(C \rightarrow \infty)$, whereas the uncertainty of κ/Λ , i.e., the shape of the fitted curve to the data, is only a minor contribution to $\Delta Q(C \rightarrow \infty)$. The results are compiled in Table II for both data sets I and II, independently.²⁷

Furthermore, we performed a common fit, denoted I+II, which contains both data sets I and II. The result of this fit is

$$\Lambda = 0.65 \pm 0.07,$$

$$\kappa = 1.40 \pm 0.22,$$

which is closer to the one obtained from data set I governed by the size of the error bars. $\kappa/\Lambda = 2.2 \pm 0.4$ and $Q(C \rightarrow \infty) = (32 \pm 3)\%$ are again in very good agreement with the individual fits. The result of this fit is also listed in Table II and drawn in Fig. 6 as a solid line.

The parameters Λ , κ , the ratio κ/Λ , and $Q(C \rightarrow \infty)$ are listed in Table II along with the old results from Petrukhin and Prokoshkin.¹¹ Our value for $Q(C \rightarrow \infty)$ is somewhat larger than Petrukhin's value, but the values of Λ and κ are consistent. For a more direct comparison between our results and Petrukhin's we have extracted the results for $Q(C)$ from Ref. 11 and have attempted a fit with MINUIT resulting in $\Lambda = 0.49 \pm 0.09$ and $\kappa = 1.44 \pm 0.37$ compared to $\Lambda = 0.4 \pm 0.1$ and $\kappa = 1.3 \pm 0.4$ from their least-squares fit. Consequently, $\kappa/\Lambda = 2.9 \pm 0.9$ and $Q(C \rightarrow \infty) = 25\%$, which is even closer to our results. This should be viewed with some caution, however, as we extracted the data points from a figure in Ref. 11 (the data were not presented in tabular form). It is also not clear whether all the data were included in the fit given in Ref. 11. Finally, it becomes evident from the fitting that the two parameters Λ and κ are correlated and the minimum in the χ^2 surface found by MINUIT is

TABLE II. Comparison of the fit parameters. I and II denote our data sets I and II, respectively, I+II is a common fit of both data sets. The world fit comprises our data as well as the data by Aniol *et al.* (Ref. 8) and Kravtsov *et al.* (Ref. 23).

Parameter	Present measurement		Petrukhin and Prokoshkin ^a	World fit
Λ	I	0.71±0.09	0.4±0.1	0.45±0.04
	II	0.40±0.10		
	I+II	0.65±0.07		
κ	I	1.56±0.28	1.3±0.4	0.93±0.14
	II	0.91±0.20		
	I+II	1.40±0.22		
κ/Λ	I	2.2±0.5	3.3±1.3	2.1±0.4
	II	2.3±0.8		
	I+II	2.2±0.4		
$Q(C \rightarrow \infty)$	I	(31±3)%	(23±4)%	(33±3)%
	II	(30±4)%		
	I+II	(32±3)%		

^aReference 11.

very shallow. Our values for κ agree within the fairly large error bars with Petrukhin, but we observe somewhat more pion transfer as emphasized by $Q(C \rightarrow \infty)$. Petrukhin's conclusions that pion capture exceeds pion transfer in π^-p+d collisions is reflected by the ratio $\kappa/\Lambda > 1$ and also holds for our observations. $\kappa > 1$ suggests that pion capture in hydrogen is more probable in π^-p+d collisions than in π^-p+p collisions. However, from the summary of all fits it appears that the value for κ is rather close to 1.

Measurements by Aniol *et al.*⁸ and Kravtsov *et al.*²³ achieved higher precision for pion transfer in H₂ and D₂ gas mixtures. Both experiments were done at similar concentrations, i.e., $C \sim 1$, but in addition the density of the target was also varied. Their experimental points are listed in Table III and compared to our values obtained from the fit I+II. There is overall agreement between these experiments.

Although the claimed uncertainty for the observed transfer is smaller in Refs. 8 and 23, the conclusions which can be drawn from data with one concentration only are limited. However, we would like to point out that both experiments are of considerable interest in a somewhat different context. The experimental investigations by Aniol *et al.*⁸ concentrated on the study of

TABLE III. Comparison of $W_{H_2D_2}$ and $Q(C)$ around $C = 1$ for different measurements. Our values are deduced from the fit I+II using Eq. (7).

Measurement	C	$W_{H_2D_2}$	$Q(C)$
Present data	0.84	0.434±0.033	0.201±0.061
	1.0	0.393±0.034	0.214±0.068
	1.2	0.352±0.033	0.226±0.073
Aniol <i>et al.</i>	1.0	0.417±0.004	0.166±0.008
Kravtsov <i>et al.</i>	0.84	0.460±0.008	0.153±0.015
	1.2	0.385±0.005	0.188±0.010

molecular effects, observing different transfer probabilities in a $C = 1$ mixture of H₂ and D₂ compared to HD, resulting in $W_{H_2D_2}(C=1)/W_{HD} = 1.23 \pm 0.03$. Kravtsov *et al.*²³ have mainly studied pion transfer theoretically, while their data points at $C \sim 1$ for H₂+D₂ confirmed the result of Aniol *et al.* The calculations of Kravtsov *et al.* include absolute pion transfer rates for different excited states as a function of the π^-p kinetic energy. These results can be directly compared to muonic transfer rates. It is interesting to note that the calculated pion transfer rate for $n=4,5$ produces best agreement with the measured transfer probability for a kinetic energy of pionic hydrogen of ~ 1 eV. This value is in partial agreement with a recent experiment at the Swiss Institute for Nuclear Research,²⁸ measuring the pion mass difference $m_{\pi^-} - m_{\pi^0}$ in the reaction $\pi^-p \rightarrow \pi^0n$. The analysis of the neutron time-of-flight spectra also delivered a result for the kinetic energy of π^-p , determined to be ~ 1 eV with a flat tail up to 50 eV. This tail is suggested as coming from capture which occurs immediately following an atomic deexcitation. Again this result is challenging in the context of cascade calculations of pionic hydrogen.

To account for all recent data on pion transfer from π^-p to π^-d we have tried a fit including our data sets I and II as well as the points from Aniol *et al.* and Kravtsov *et al.* The result of this "world fit" is

$$\Lambda = 0.45 \pm 0.04,$$

$$\kappa = 0.93 \pm 0.14,$$

with $\kappa/\Lambda = 2.1 \pm 0.4$ and $Q(C \rightarrow \infty) = (33 \pm 3)\%$. The result of this fit is drawn as a solid line in Fig. 7, where all data are displayed. The solid circles are our present values, which for clarity are plotted for $C > 2$ only, the open squares are from Petrukhin and Prokoshkin, whose fit is drawn as a dashed line too, the solid square is the datum from Aniol *et al.*, and the diamonds are from Kravtsov *et al.* From Fig. 7 it becomes very obvious that our data points provide new information for $C > 3$, ex-

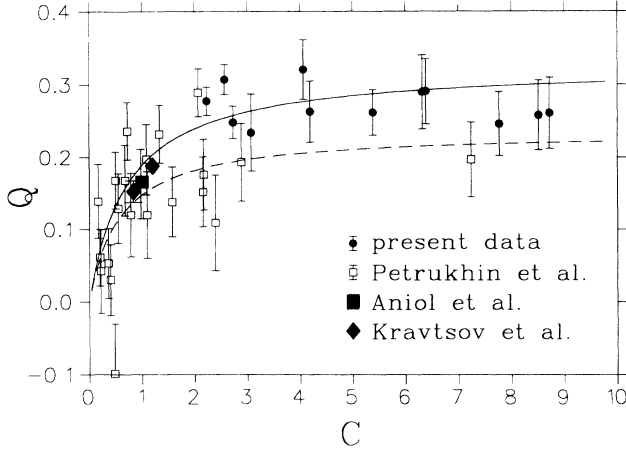


FIG. 7. Transfer probability Q as a function of C . The solid circles are data from the present measurement with $C > 2$ only for clarity (for a full account of our data see Fig. 6 or Table I), the open squares are from Petrukhin and Prokoshkin, the solid square is the datum from Aniol *et al.*, and the diamonds are from Kravtsov *et al.* The solid line is the result from the “world fit,” the dashed line is the fit from Petrukhin and Prokoshkin. The function $Q = \Lambda C / (1 + \Lambda C + \kappa C)$ has been fitted to the data with $\Lambda = 0.45$ and $\kappa = 0.93$ for the “world fit,” and $\Lambda = 0.40$ and $\kappa = 1.30$ for Petrukhin’s fit.

cept for the one datum at $C \sim 7$ by Petrukhin and Prokoshkin. Needless to say, the information at large C is essential to determine the asymptotic value $Q(C \rightarrow \infty)$.

The transfer probability is of interest in muon-catalyzed fusion. Of particular interest is the term called Q_{1s} , which is the probability of a muon reaching the ground state of the $d\mu$ atom before transferring to a triton. From an analysis of the muon recycling rates it has turned out to be difficult to extract Q_{1s} unambiguously²⁹ because Q_{1s} is combined with several other parameters. From our data and the experimental and theoretical estimates of the time scales in Fig. 1 we can obtain a value for λ_{pd} . Experiments¹⁴ show that the mean lifetime of a π^- in liquid hydrogen between the time when its velocity is $\approx 0.006c$ and the time of nuclear capture is $(2.3 \pm 0.6) \times 10^{-12}$ s. Without any further theoretical and experimental guidance we can set a lower limit on the transfer rate if we assume that almost all of the 2.3×10^{-12} s is spent in $(\pi^- p)_n$ states. From Eq. (8), as $C_d \rightarrow 1$, we solve for λ_{pd} and obtain

$$\lambda_{pd} = \beta_{pd} \left[\frac{Q}{1-Q} \right]. \quad (14)$$

Now $Q = (32 \pm 3)\%$, and if we use $\beta_{pd} = \beta_{pp}$ (consistent with $\kappa = 1$) we conclude that

$$\beta_{pd} = \frac{1}{2.3 \times 10^{-12}}, \quad (15)$$

so

$$\lambda_{pd}^{\min} = (2.0 \pm 0.5) \times 10^{11}, \quad (16)$$

both in s^{-1} . This is the smallest value of λ_{pd} because on

theoretical grounds^{23,30} one expects the transfer to be significant only once the $(\pi^- p)_n$ atom has reached $n=4,5$. Using various theoretical estimates^{31,32} one can estimate that a mean time of about 1.3×10^{-12} s is required from the free π^- to the $(\pi^- p)_{n=4,5}$ states. Hence nuclear capture from these states occurs in a time less than about 1×10^{-12} s. This means that a more likely value of λ_{pd} is

$$\lambda_{pd} = (4.7 \pm 1.5) \times 10^{11}, \quad (17)$$

in s^{-1} . This rate agrees with a previously published value³³ of $(6 \pm 3) \times 10^{11} s^{-1}$ from an experiment in liquid $H_2 + D_2$ mixtures. Note that the above analysis assumed that our results can be extrapolated to liquid hydrogen densities. It is interesting to compare this value of λ_{pd} with an analogous rate calculated³⁴ for $(d\mu)_n + t \rightarrow d + (\mu t)_n$. For $n=4$ these authors calculate a transfer rate of $4.8 \times 10^{11} s^{-1}$ at a muon kinetic energy of 1.0 eV.

The pressure dependence of π^- transfer has been investigated for $C=1.216$. $W_{H_2D_2}$ was determined to be 0.350 ± 0.010 , 0.365 ± 0.012 , and 0.375 ± 0.014 for 100, 66, and 33 atm, respectively. The results agree well within the error bars, exhibiting no pressure dependence, which is in accord with earlier observations.⁸ This observation is an important test of the phenomenological model, as relation (6) does not suggest any pressure dependence.

VI. SUMMARY AND CONCLUSIONS

In this experiment the concentration dependence of π^- transfer has been studied in gas mixtures of H_2 and D_2 . The measured concentration dependence has important impact on similar studies related to muon-catalyzed fusion. The data have been fitted to a phenomenological model with two parameters. The results of the fits are as follows.

(i) The maximum transfer $Q(C \rightarrow \infty)$ amounts to $(32 \pm 3)\%$, which is somewhat higher than that observed in the previous measurement by Petrukhin and Prokoshkin.¹¹

(ii) The ratio of the two fitted parameters $\kappa/\Lambda > 1$ confirms that in $\pi^- p + d$ collisions the capture probability is higher than the transfer reaction.

(iii) The inverse transfer reaction $\pi^- d + p \rightarrow \pi^- p + d$ cannot be discarded definitely by our measurement because the uncertainty of the parameter Λ is too large and the theoretical predictions too vague.

(iv) Since $\kappa \sim 1$, pion capture in hydrogen has similar probabilities in $\pi^- p + d$ collisions and in $\pi^- p + p$ collisions.

Both fitted parameters Λ and κ are very sensitive to the shape of $Q(C)$, as indicated by the error bars in Table II. Therefore the conclusions drawn from either Λ or κ have to be handled with some care, the more so since assumptions were made for the formulation of the phenomenological model. It appears that $Q(C \rightarrow \infty)$ is a more stable number and its value can be estimated in measurements with large concentrations C , independent of the phenom-

enological model. The data for $C \sim 1$ mixtures of H_2 and D_2 are in overall agreement with the precision experiments of Aniol *et al.*⁸ and Kravtsov *et al.*²³

The pressure dependence of π^- transfer has been investigated for one concentration ($C=1.216$) and no effect was found in accord with the description of the phenomenological model and previous measurements. In an auxiliary experiment the charge exchange probability in nitrogen was investigated. An upper limit of 7×10^{-5}

(90% confidence level) was found for the π^0 production in N_2 .

ACKNOWLEDGMENTS

This work was supported jointly by the Natural Sciences and Engineering Research Council of Canada, the National Research Council of Canada, and (M.R.H.) the United Kingdom Science and Engineering Research Council.

*Present address: Virginia Polytechnic Institute and State University, Blacksburg, VA 24061.

†Present address: Los Alamos National Laboratory, Mail Stop H846, Los Alamos, NM 87545.

¹L. I. Ponomarev, *Annu. Rev. Nucl. Sci.* **23**, 395 (1973).

²D. Horváth, *Radiochim. Acta A* **28**, 241 (1981).

³H. Schneuwly, V. N. Pokrovsky, and L. I. Ponomarev, *Nucl. Phys.* **A312**, 419 (1978).

⁴H. Daniel, *Z. Phys. A* **291**, 29 (1979).

⁵T. von Egidy, D. H. Jakubassa-Amundsen, and F. J. Hartmann, *Phys. Rev. A* **29**, 455 (1984).

⁶L. I. Ponomarev, *Yad. Fiz.* **2**, 223 (1965) [*Sov. J. Nucl. Phys.* **2**, 160 (1966)]; **6**, 389 (1967) [**6**, 281 (1968)]; L. I. Ponomarev and Yu. D. Prokoshkin, *Comments Nucl. Part. Phys.* **2**, 176 (1968).

⁷S. S. Gershtein, V. I. Petrukhin, L. I. Ponomarev, and Yu. D. Prokoshkin, *Usp. Fiz. Nauk.* **97**, 3 (1969) [*Sov. Phys.—Usp.* **12**, 1 (1970)].

⁸K. A. Aniol, D. F. Measday, M. D. Hasinoff, H. W. Roser, A. Bagheri, F. Entezami, C. Virtue, J. M. Stadlbauer, D. Horváth, M. Salomon, and B. C. Robertson, *Phys. Rev. A* **28**, 2684 (1983).

⁹V. I. Petrukhin, Yu. D. Prokoshkin, and V. M. Suvorov, *Zh. Eksp. Teor. Fiz.* **55**, 2173 (1968) [*Sov. Phys.—JETP* **28**, 1151 (1969)].

¹⁰V. I. Petrukhin and V. M. Suvorov, *Zh. Eksp. Teor. Fiz.* **70**, 1145 (1976) [*Sov. Phys.—JETP* **43**, 595 (1976)].

¹¹V. I. Petrukhin and Yu. D. Prokoshkin, *Zh. Eksp. Teor. Fiz.* **56**, 501 (1969) [*Sov. Phys.—JETP* **29**, 274 (1969)].

¹²N. Imanishi, Y. Takeuchi, K. Toyoda, A. Shinohara, and Y. Yoshimura, *Nucl. Instrum. Methods A* **261**, 465 (1987).

¹³V. A. Vasilyev, B. Lévy, A. Minkova, V. I. Petrukhin, and D. Horváth, *Nucl. Phys. A* **446**, 613 (1985).

¹⁴J. H. Doede, R. H. Hildebrand, M. H. Israel, and M. R. Pyka, *Phys. Rev.* **129**, 2808 (1963).

¹⁵A. V. Bannikov, B. Lévy, V. I. Petrukhin, V. A. Vasilyev, L. M. Kochenda, A. A. Markov, V. I. Medvedev, G. L. Sokolov, I. I. Strakovsky, and D. Horváth, *Nucl. Phys. A* **403**, 515 (1983).

¹⁶L. I. Ponomarev, *Atomkernenergie—Kerntechnik* **43**, 175 (1983).

¹⁷S. E. Jones, A. N. Anderson, A. J. Caffrey, C. DeW. Van Sclen, K. D. Watts, J. N. Bradbury, J. S. Cohen, P. A. M. Gram, M. Leon, M. R. Maltrud, and M. A. Paciotti, *Phys. Rev. Lett.* **56**, 588 (1986).

¹⁸L. I. Menshikov, *Muon Catalyzed Fusion* **2**, 173 (1988).

¹⁹J. Spuller, D. Berghofer, M. D. Hasinoff, R. MacDonald, D. F. Measday, M. Salomon, T. Suzuki, J.-M. Poutissou, R. Poutissou, and J. K. P. Lee, *Phys. Lett.* **67B**, 479 (1977).

²⁰G. Backenstoss, M. Izycki, W. Kowald, P. Weber, H. J. Weyer, S. Ljungfelt, U. Mankin, G. Schmidt, and H. Ullrich, *Nucl. Phys.* **A448**, 567 (1986).

²¹B. Bassalleck, F. Corriveau, M. D. Hasinoff, T. Marks, D. F. Measday, J.-M. Poutissou, and M. Salomon, *Nucl. Phys.* **A362**, 445 (1981).

²²R. MacDonald, D. S. Beder, D. Berghofer, M. D. Hasinoff, D. F. Measday, M. Salomon, J. Spuller, T. Suzuki, R. Poutissou, J.-M. Poutissou, P. Depommier, and J. K. P. Lee, *Phys. Rev. Lett.* **38**, 746 (1977).

²³A. V. Kravtsov, A. Yu. Mayorov, A. I. Mikhailov, S. Yu. Ovchinnikov, N. P. Popov, V. M. Suvorov, and A. I. Shchetkovsky, *Muon Catalyzed Fusion* **2**, 199 (1988).

²⁴D. Horváth, K. A. Aniol, F. Entezami, D. F. Measday, A. J. Noble, S. Stanislaus, C. J. Virtue, A. S. Clough, D. F. Jackson, J. R. H. Smith, and M. Salomon (unpublished).

²⁵J. F. Bartlett, J. R. Briel, D. B. Curtis, R. J. Dosen, T. D. Lagerhund, E. K. Quigg, D. J. Ritchie, and L. M. Taff, computer program MULTI (Fermilab); TRIUMF implementation by Y. Miles.

²⁶F. James and M. Roos, *Comput. Phys. Commun.* **10**, 343 (1975).

²⁷If the single data point heretofore discarded is included in the analysis of data set I, the result is $\Lambda=0.91$, $\kappa=2.42$, and $Q(C \rightarrow \infty)=27.4\%$ with a very poor $\chi^2/df=7.3$. Note that while Λ and κ change considerably, $Q(C \rightarrow \infty)$ is only slightly reduced by the inclusion of this point.

²⁸J. F. Crawford, M. Daum, R. Frosch, B. Jost, P.-R. Kettle, R. M. Marshall, B. K. Wright, and K. O. H. Ziock, *Phys. Lett.* **213B**, 391 (1988).

²⁹A. N. Anderson, in *Muon-Catalyzed Fusion*, Proceedings of a conference on Muon-Catalyzed Fusion, Sanibel Island, Florida, 1988, AIP Conf. Proc. No. 181, edited by S. E. Jones, J. Rafelski, and H. J. Monkhorst (AIP, New York, 1989).

³⁰A. V. Kravtsov, A. I. Mikhailov, S. Yu. Ovchinnikov, and N. P. Popov, *Muon Catalyzed Fusion* **2**, 183 (1988).

³¹T. B. Day, G. A. Snow, and J. Sucher, *Phys. Rev. Lett.* **3**, 61 (1959).

³²M. Leon and H. Bethe, *Phys. Rev.* **127**, 676 (1962).

³³K. Derrick, M. Derrick, J. C. Fetkovich, T. H. Fields, E. G. Pewitt, and G. B. Yodh, *Phys. Rev.* **151**, 82 (1966).

³⁴L. I. Menshikov and L. I. Ponomarev, *Z. Phys. D* **2**, 1 (1986).

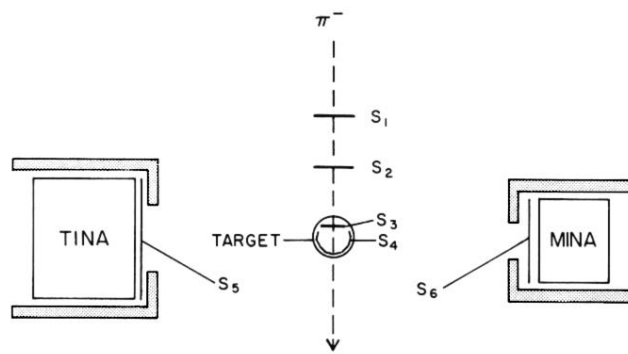


FIG. 2. Experimental setup. S_1 – S_6 are plastic scintillation counters. TINA and MINA are the NaI crystals detecting the γ rays from the π^0 decay. The boxes around TINA and MINA shield from background and define the aperture.